ICIC Express Letters
Part B: Applications
Volume **14**, Number **8**, August **2023**

ICIC International ©2023 ISSN 2185-2766
pp. **847–854**

MULTI-AUV CIRCULAR FORMATION CONTROL BASED ON VIRTUAL LEADER

Juan Li[1,2], Yanxin Zhang[2], Honghan Zhang[1,2] and Xinnian Chen[2]

[1]Science and Technology on Underwater Vehicle Technology Laboratory
[2]College of Intelligent Systems Science and Engineering
Harbin Engineering University
No. 145, Nantong Street, Nangang District, Harbin 150001, P. R. China
{ Lijuan041; zhanyanxin; chenxinnian }@hrbeu.edu.cn; zhanghonghan2008@163.com

Received December 2022; accepted February 2023

Abstract. *This paper presents a multi-AUV circular formation control method based on virtual leader. Firstly, the second-order linear model of AUV is obtained by precise feedback linearization method, and an adaptive sliding mode AUV trajectory tracking controller is designed. AUV circular formation is generated by virtual leader formation control method. Finally, the simulation results verify the effectiveness of the method.*
Keywords: Feedback linearization, Adaptive sliding mode, AUV circular formation, Virtual leader

1. **Introduction.** AUV (autonomous underwater vehicle) does not rely on the mother ship to provide power, and has strong mobility, wide range of activities, and high operational efficiency [1], making it gradually become the main research object of researchers in various countries. Its various technologies have been well developed, and have been well applied in civil and military fields such as marine resource exploration, investigation and surveillance, and anti-submarine. With the development and maturity of underwater unmanned submersible technology, single autonomous underwater vehicle has been unable to meet the needs of the development, which makes multi-autonomous underwater vehicle in the form of cluster collaborative task has become an inevitable trend in the development of underwater unmanned submersibles.

In recent years, the multi-intelligent circular formation control problem has attracted many scholars to study. For the multi-AUV moving-target hunting or collaborative searching tasks, multi-AUV round-up areas or search areas are required to be as large as possible. At this time, the circular formation is highly expandable, and the coverage area is large [2]. Wang et al. [3] investigate the circular formation control problem of car-like robots with limited sensing range. Xu et al. [4] investigate circular formation control problems for a group of anonymous mobile robots in the plane, where all robots can converge asymptotically to a predefined circular orbit around a fixed target point without collision, and maintain any desired relative distances from their neighbors. Sun et al. [5] discuss the problem of controlling formation shapes for a group of nonholonomic unicycle-type agents with constant speeds. The circular motion center is adopted as a virtual position for each agent to define the desired formation shape. Marshall et al. [6] apply the classical nonlinear cyclic tracking theory to the wheeled vehicle system with unicycle model, and the vehicle formation finally forms a circular formation with the geometric center of mass at the initial position as the center of the circle. The local stability of the balanced regular polygon formed by the line of trolleys in a circular formation is analyzed. Chen et al. [7] propose a new distributed formation flight protocol for unmanned aerial vehicles (UAVs) to perform coordinated circular tracking around a set of circles on a target sphere. The

DOI: 10.24507/icicelb.14.08.847

proposed multi-AUV circular formation based on virtual leader has practical significance for the capture of moving targets in the ocean. The formation control method using virtual leader greatly reduces the dependence of formation members on the leader and improves the formation flexibility.

This paper presents a multi-AUV circular formation control method based on virtual leader. The rest of this article is organized as follows. In Section 2, the AUV nonlinear model is transformed into a second-order linear model by using the precise feedback linearization method. In Section 3, an adaptive sliding-film trajectory tracking controller is designed and the stability of the controller is analyzed. In Section 4, a circular formation controller based on virtual leader is proposed. In Section 5, the performance of the controller is verified by simulation. Section 6 is the summary of the article.

2. **Construction of AUV Feedback Linearization Model.** Feedback linearization control is to apply state feedback to the nonlinear system so that the closed loop system becomes linear. In [8], the microgrid secondary voltage control is transformed into a linear second-order tracker synchronization problem by feedback linearization. Aiming at the problem that the nonlinear and strong coupling model of AUV leads to the difficulty of controller design, the nonlinear model is linearized by feedback linearization method, then the complex model is transformed into a linear second-order integral model, and the system error of the nonlinear model is eliminated.

In Figure 1, E-$\xi\eta\zeta$ is the northeast coordinate system, i.e., the fixed coordinate system, and O-xyz is the hull coordinate system, i.e., the inertial coordinate system. The detailed mathematical model of the AUV is built as follows.

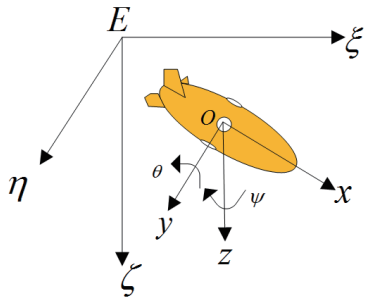

FIGURE 1. AUV coordinate diagram

The AUV is full-actuated. The following dynamics and kinematics model is developed in the body coordinate system:

$$\begin{cases} \dot{\eta} = J(\eta)v \\ M\dot{v} = g'\tau - C(v)v - D(v)v - g(\eta) \end{cases} \tag{1}$$

In the model, $\eta = (x, y, z, \theta, \psi)^T \in R^5$ is position vector of the AUV in the fixed coordinate system. The velocity vector of the AUV in the hull coordinate system is $v = (u, v, w, q, r)^T \in R^5$. M is the inertial matrix and $J(\eta)$ is the transition matrix. $C(v)$ is the Coriolis and centripetal force matrices. $D(v)$ is the lifting force moment and hydrodynamic drag. The restoring force and torque vector is $g(\eta)$. The input vector of the AUV actuator is $\tau = (\tau_u, \tau_v, \tau_w, \tau_q, \tau_r)^T \in R^5$ and $g' \in R^{5\times5}$ is the parameter matrix of the actuator. The higher order damping term and the effect of hull swing on the AUV motion are not considered.

Kinematic model:

$$\begin{cases} \dot{x} = u\cos\psi\cos\theta - v\sin\psi + w\cos\psi\sin\theta \\ \dot{y} = u\sin\psi\cos\theta + v\cos\psi + w\sin\psi\sin\theta \\ \dot{z} = -u\sin\theta + w\cos\theta \\ \dot{\theta} = q \\ \dot{\psi} = r/\cos\theta \end{cases} \tag{2}$$

The AUV model is appropriately transformed for the subject in this paper:

$$\begin{cases} \dot{\eta} = J(\eta)v \\ \dot{v} = M^{-1}g'\tau + M^{-1}N(\eta, v) \end{cases} \tag{3}$$

The above (3) is transformed into the following form for the model linearization:

$$\dot{\xi} = f(\xi) + M_1 g'\tau \tag{4}$$

The output quantity of the nonlinear system is the position vector, and the nonlinear model of the AUV is as follows:

$$\begin{cases} \dot{\xi} = f(\xi) + g(\xi)\tau \\ \varsigma = h(\xi) \end{cases} \tag{5}$$

In the model, $f(\xi) = M_1 \begin{bmatrix} J(\eta)v & N(\eta, v) \end{bmatrix}^T$, $g(\xi) = M_1 g'$, $h(\xi) = (x, y, z, \theta, \psi)^T$.
It can be seen from the definition of the Lie derivative in [9]:

$$\dot{\varsigma} = \frac{\partial h}{\partial \xi}(f(\xi) + g(\xi)) \tag{6}$$

The first Lie derivative $L_f^2 h(\xi)$, $L_g L_f h(\xi)$ can be obtained with the following form:

$$\begin{cases} L_f h(\xi) = J(\eta)v \neq 0 \\ L_g h(\xi) = 0 \end{cases} \tag{7}$$

Similarly, according to the definition of the second-order Lie derivative, we can obtain

$$\ddot{\varsigma} = \frac{\partial L_f h(\xi)}{\partial \xi}(f(\xi) + g(\xi)\tau) \tag{8}$$

While the second-order Lie derivative has the following form:

$$\begin{cases} L_f^2 h(\xi) = \dfrac{\partial L_f h(\xi)}{\partial \xi} f(\xi) \neq 0 \\ L_g L_f h(\xi) = \dfrac{\partial L_f h(\xi)}{\partial \xi} g(\xi) \neq 0 \end{cases} \tag{9}$$

According to the definition in [9], the sum of the relative orders of the model is

$$\rho_1 + \rho_2 + \rho_3 + \rho_4 + \rho_5 = 10 \tag{10}$$

where $\rho_1 = \rho_2 = \rho_3 = \rho_4 = \rho_5 = 2$, that is, the sum of the relative order is equal to the order of the system (10). It can be seen that the AUV model can be accurately feedback linearized and has a solution.

Select coordinate changes as follows:

$$\begin{cases} z_1(\xi) = (h_1(\xi), h_2(\xi), h_3(\xi), h_4(\xi), h_5(\xi))^T \\ z_2(\xi) = (L_f h_1(\xi), L_f h_2(\xi), L_f h_3(\xi), L_f h_4(\xi), L_f h_5(\xi))^T \end{cases} \tag{11}$$

And

$$\begin{cases} \dot{z}_1 = z_2 \\ \dot{z}_2 = L_f^2 h(\xi) + L_g L_f h(\xi)\tau \end{cases} \tag{12}$$

If $U = L_f^2 h(\xi) + L_g L_f h(\xi)\tau$, then the actual control input under a new coordinate transformation is as follows: $\tau = (L_g L_f h(\xi))^{-1}(U - L_f^2 h(\xi))$.

The AUV linearized mathematical model of AUV is obtained as

$$\begin{cases} \dot{z}_1 = z_2 \\ \dot{z}_2 = U \end{cases} \tag{13}$$

At this time, the construction of the AUV linearized model is achieved.

3. **AUV Trajectory Tracking Control.** In this paper, the method of sliding mode control is used to realize AUV 3D trajectory tracking control under steady ocean current environment.

Assumption 3.1. *The desired trajectory of AUV η_d is smooth and bounded, $\dot{\eta}_d$ and $\ddot{\eta}_d$ are also bounded.*

Assumption 3.2. *Ocean current disturbances are always bounded.*

Set η_d as the desired motion track, it is assumed that the ocean current disturbance is steady, the ocean current size is v m/s, the flow direction angle is α, then $z_{1d}(t) = \eta_d(t)$, $z_{1e}(t) = z_1(t) - z_{1d}(t)$, $z_{2e}(t) = z_2(t) - z_{2d}(t) + v_{dis}$, in the inertial coordinate system, the influence of ocean current disturbance on AUV velocity is

$$\begin{cases} u_c = v * (\cos\alpha\cos\psi + \sin\alpha\sin\psi) \\ v_c = v * (-\cos\alpha\sin\psi + \sin\alpha\cos\psi) \\ v_{dis} = (u_c, v_c, 0, 0, 0)^T \end{cases} \tag{14}$$

where u_c is the amount of interference of ocean current disturbance to AUV longitudinal velocity, and v_c is the amount of interference of ocean current disturbance to AUV transverse velocity.

Defining the sliding surface:

$$s = k_1 z_{1e}(t) + k_2 z_{2e}(t) \tag{15}$$

where $\dot{z}_{1e}(t) = z_{2e}(t)$, $\dot{z}_{2e}(t) = U(t)$, take first derivative of t of (15), we can obtain

$$\dot{s} = k_1 z_{2e}(t) + k_2 U(t) \tag{16}$$

where $k_1, k_2 > 0$, taking the exponential approach rate:

$$\dot{s} = -ks - \varepsilon \mathrm{sgn}(s) \tag{17}$$

where k is the constant velocity approach coefficient, $k > 0$, ε is the exponential approach coefficient. $\varepsilon = k_3|s_i|$, $0 \le k_3 < 1$ and $\varepsilon > 0$. Substituting (17) into (16), the control quantity U can be obtained:

$$U(t) = (-kk_1 z_{1e}(t) - (kk_2 + k_1) z_{2e}(t) - \varepsilon \mathrm{sgn}(s))/k_2 \tag{18}$$

Through simulation and data reference, it is found that the controller obtained by taking this approach rate can achieve stability and convergence, but it will bring continuous periodic chattering, which cannot achieve the stable output of the actuator. Therefore, the chattering caused by the sliding mode controller can be eliminated by designing an adaptive variable parameter method.

Let $\varepsilon = k_3|s|$, where $|s|$ is the modulus of the sliding surface, $0 \le k_3 < 1$, and ε is proportional to $|s|$. When the system state is far from the sliding surface, ε will be larger, which can shorten the time of stable convergence of the system. When approaching the sliding surface, ε is infinitely close to zero, and the chattering-free sliding mode control is realized.

Taking ε into (18), the final virtual control quantity can be obtained:

$$U(t) = (-kk_1 z_{1e}(t) - (kk_2 + k_1) z_{2e}(t) - k_3|s|\mathrm{sgn}(s))/k_2 \tag{19}$$

The following is proof of controller stability.

The Lyapunov function is selected as follows:

$$y = \frac{1}{2}s^T s \tag{20}$$

The derivative of the first order of the above formula is

$$\dot{y} = s^T \dot{s} = (k_1 z_{1e}(t) + k_2 z_{2e}(t))^T (k_1 z_{2e}(t) + k_2 U(t)) \tag{21}$$

Substituting (19) into (21), we can get

$$\begin{aligned}\dot{y} &= (k_1 z_{1e}(t) + k_2 z_{2e}(t))^T [k_1 z_{2e}(t) + k_2((-kk_1 z_{1e}(t) - (kk_2 + k_1) z_{2e}(t) - k_3 |s|\mathrm{sgn}(s))/k_2)] \\ &= (k_1 z_{1e}(t) + k_2 z_{2e}(t))^T [-kk_1 z_{1e}(t) - kk_2 z_{2e}(t) - k_3 |s|\mathrm{sgn}(s)] \\ &= -k(k_1 z_{1e}(t) + k_2 z_{2e}(t))^T (k_1 z_{1e}(t) + k_2 z_{2e}(t)) - k_3 s^T |s|\mathrm{sgn}(s) \\ &= -k_1 s^T s - k_3 s^T s \leq 0 \end{aligned} \tag{22}$$

It can be seen from (20) that Lyapunov function is positive definite, and from (22) that the derivative of Lyapunov function is negative definite. Therefore, under the action of control input (19), the closed-loop system is stable and convergent, and the following simulation experiment also verified the stability of the controller.

4. **AUV Circular Formation Control.** Formation requirements: The circular formation can be realized based on the virtual leader, and the formation can be maintained in a three-dimensional space. The formation is shown in Figure 2.

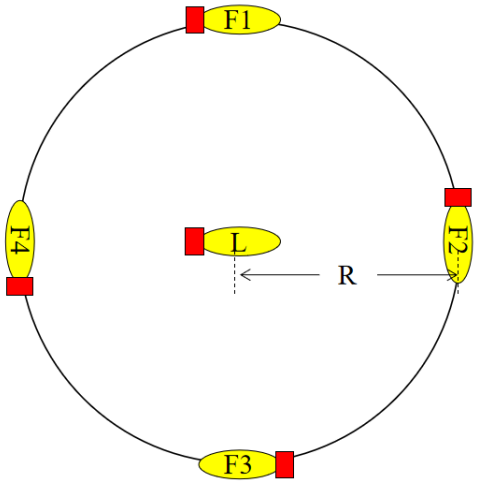

FIGURE 2. Schematic diagram of formation

In Figure 2, L represents the virtual leader, and F1, F2, F3 and F4 are the followers of the AUV, respectively. If the formation is constrained by the constraint quantity in the schematic diagram, the formation cannot be maintained through a traditional constraint mode in a three-dimensional space. This paper proposes the following constraint method:

$$\begin{cases} \eta_L + d_i = \eta_{Fi} \\ \dot{\eta}_L + dv_i = \dot{\eta}_{Fi} \end{cases} \quad i = 1, 2, \ldots, n \tag{23}$$

η_L is the motion state of the virtual leader and η_{Fi} is the motion state vector between the virtual leader and follower i.

$$\begin{cases} d_i = (R\cos(\psi_L + (i-1)\beta), R\sin(\psi_L + (i-1)\beta), 0, 0, (i-1)\beta) \\ dv_i = (r_L R, 0, 0, 0, 0) \end{cases} \quad i = 1, 2, \ldots, n \tag{24}$$

R is the distance between the virtual leader and the follower, and β is the deviation of heading angle between follower and virtual leader.

If there are n AUVs in the virtual leader-follower formation, and the motion state vector of the follower i at time t is $\varepsilon_i(t) = \eta_i(t)$, then the motion state vector of the virtual leader

is $\varepsilon_L(t) = \eta_L(t)$. If (25) is satisfied, the formation maintenance and stability convergence can be realized:

$$\begin{aligned} &\lim_{t\to\infty} |\varepsilon_i(t) - \varepsilon_L(t) + d_i| = 0 \\ &\lim_{t\to\infty} |\dot{\varepsilon}_i(t) - \dot{\varepsilon}_L(t) + dv_i| = 0 \end{aligned} \qquad i = 1, 2, \ldots, n \tag{25}$$

If $z_{1d}(t) = \eta_L$ and $z_{2d}(t) = V_L$, η_L and V_L are the attitude vector and velocity vector of the virtual leader, then the two input deviations can be expressed as

$$\begin{cases} z_{i1e}(t) = z_{i1}(t) - z_{1d}(t) - d_i \\ z_{i2e}(t) = z_{i2}(t) - z_{2d}(t) - dv_i \end{cases} \tag{26}$$

Defining the sliding surface:

$$s_i = k_1 z_{i1e}(t) + k_2 z_{i2e}(t) \tag{27}$$

where $\dot{z}_{i1e}(t) = z_{i2e}(t)$, $\dot{z}_{i2e}(t) = U_i(t)$, take first derivative of t of (27), we can obtain

$$\dot{s}_i = k_1 z_{i2e}(t) + k_2 U_i(t) \tag{28}$$

where $k_1, k_2 > 0$, taking the exponential approach rate:

$$\dot{s}_i = -k s_i - \varepsilon \mathrm{sgn}(s_i) \tag{29}$$

where k is the constant velocity approach coefficient, $k > 0$, ε is the exponential approach coefficient. $\varepsilon = k_3|s_i|$, $0 \le k_3 < 1$ and $\varepsilon > 0$. Substituting (29) into (28), the control quantity U_i can be obtained:

$$U_i(t) = (-kk_1 z_{i1e}(t) - (kk_2 + k_1) z_{i2e}(t) - k_3 |s_i| \mathrm{sgn}(s_i))/k_2 \tag{30}$$

In the model, U is the controller input of follower i.

5. **Simulation.** The four follower AUVs were deployed in the environment, first to achieve a circular formation at the horizontal level, and then to maintain a circular formation at a depth of 30 meters. The deviation of $x_i(0)$ and $y_i(0)$ from the initial expected position $[-10, 10]$ m, the initial range of $z_i(0)$ is $[-3, 3]$ m, the initial range of initial attitude and heading angle is $[0, 1]$ rad, the initial range of longitudinal velocity is $[0, 0.5]$ m/s, all other velocities are initialized to 0 m/s, and the controller parameter is $k = 1$, $k_1 = 0.2$, $k_2 = 0.8$, $k_3 = 0.007$. Radius of circular formation $R = 60$ m, the flow velocity of the steady ocean current is 0.2 m/s, and the flow direction is 30 degrees. The simulation results are as follows.

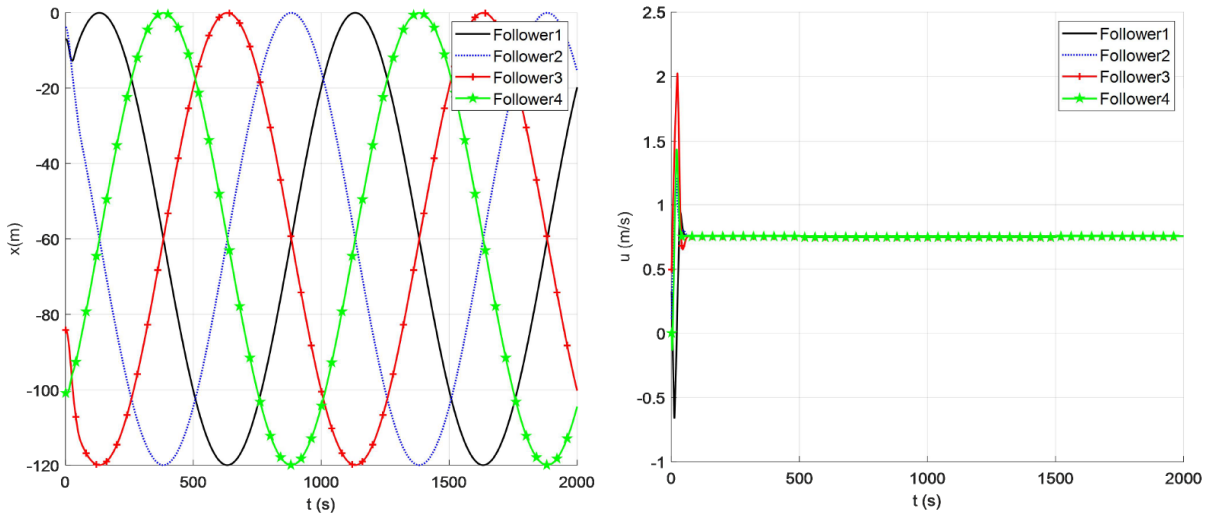

FIGURE 3. Northward displacement and longitudinal velocity of AUV

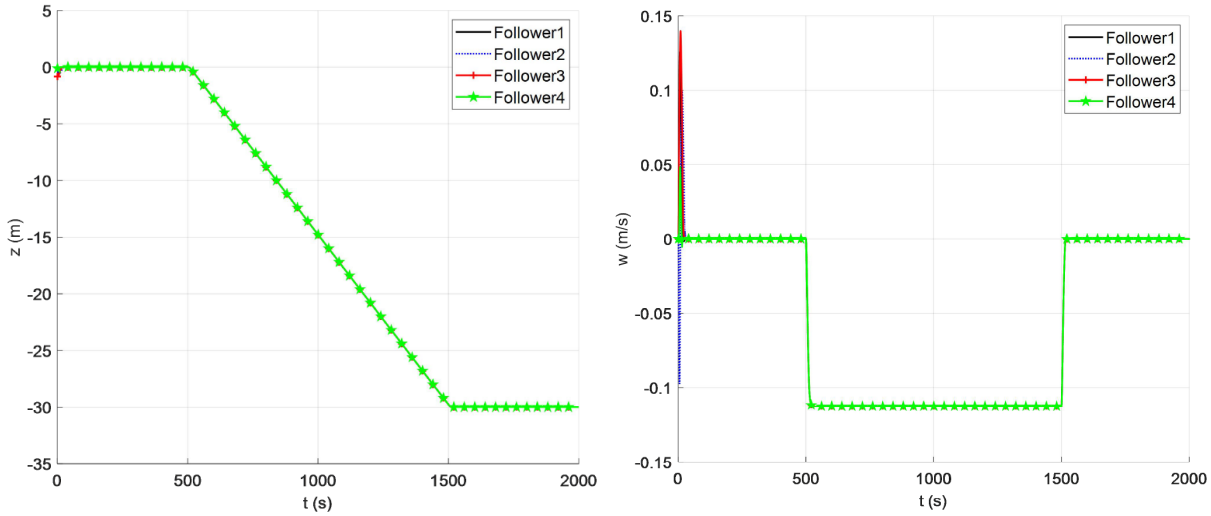

FIGURE 4. The vertical displacement and velocity of AUV

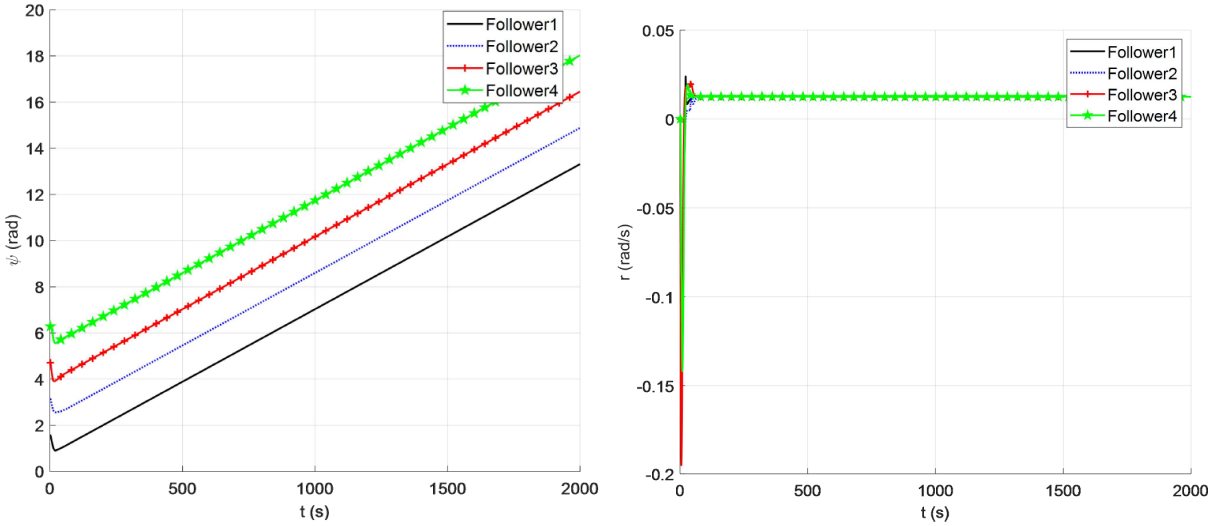

FIGURE 5. The heading angle and heading angle velocity of AUV

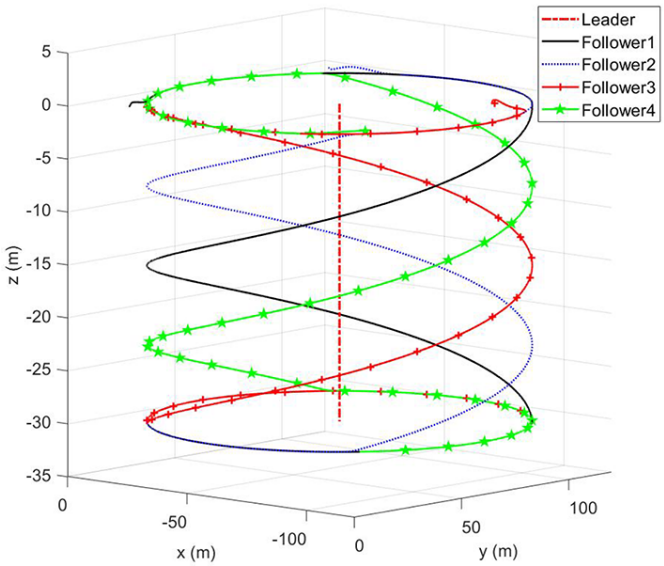

FIGURE 6. 3D trajectory of AUV

It can be seen from the three-dimensional trajectory diagram that multiple AUVs firstly form a circular formation on the horizontal plane. When the virtual leader begins to submerge, the formation members begin to submerge under the condition of maintaining the circular formation, and finally maintain at the specified depth. Although the speed of each AUV will overshoot when the formation trajectory is switched, the overshoot is also within the control range of the formation controller, and the position and speed of the AUV can track the expected value in time, which verifies that this formation controller has good control effect.

6. **Conclusions.** Starting from the nonlinear model of AUV, this paper uses the method of precise feedback linearization to construct the linearized mathematical model of AUV. Then, the sliding surface is established for the pose and velocity errors, and the adaptive variable parameter AUV sliding mode controller is given. Through the trajectory tracking simulation experiment, it is verified that the controller designed by the linear model has better control effect. Finally, based on the single controller, a multi-AUV circular formation controller is designed according to the virtual leader formation strategy. The simulation results show that the designed formation controller has good control performance and can meet the formation requirements.

The circular formation control method proposed in this paper can only be established when the virtual leader does the submarine work at a constant speed. For other motion states of the leader, further research is needed. In addition, the influence of the delay of underwater acoustic communication on formation control is not considered in this paper.

Acknowledgment. This search work was supported by the National Natural Science Foundation of China (Grant No. 5217110503 and Grant No. 51809060), the Research Fund from Science and Technology on Underwater Vehicle Technology (Grant No. JCKYS 2021SXJQR-09), and Heilongjiang Provincial Natural Science Foundation of China (Grant No. E2018023).

REFERENCES

[1] Q. Chen, *Unmanned Underwater Vehicle*, National Defense Industry Press, Beijing, 2014.
[2] G. Xia, Y. Zhang and Y. Yang, Control method of multi-AUV circular formation combining consensus theory and artificial potential field method, *2020 Chinese Control and Decision Conference (CCDC)*, pp.3055-3061, DOI: 10.1109/CCDC49329.2020.9164778, 2020.
[3] R. Wang, W. Xia and X. Sun, Circular formation control of car-like robots with local position measurements, *2018 18th International Conference on Control, Automation and Systems (ICCAS)*, pp.109-113, 2018.
[4] P. Xu et al., Distributed event-triggered circular formation control for multiple anonymous mobile robots with order preservation and obstacle avoidance, *IEEE Access*, vol.8, pp.167288-167299, 2020.
[5] Z. Sun, H. G. de Marina, G. S. Seyboth, B. D. O. Anderson and C. Yu, Circular formation control of multiple unicycle-type agents with nonidentical constant speeds, *IEEE Transactions on Control Systems Technology*, vol.27, no.1, pp.192-205, 2019.
[6] J. A. Marshall, M. E. Broucke and B. A. Francis, Formations of vehicles in cyclic pursuit, *IEEE Transactions on Automatic Control*, vol.49, no.11, pp.1963-1974, 2004.
[7] Y. Chen, R. Yu, Y. Zhang and C. Liu, Circular formation flight control for unmanned aerial vehicles with directed network and external disturbance, *IEEE/CAA Journal of Automatica Sinica*, vol.7, no.2, pp.505-516, 2020.
[8] D. Xu, Z. Cheng, W. Yang and W. Zhang, Robust nonlinear control for virtual synchronous generator based on exact feedback linearization, *International Journal of Innovative Computing, Information and Control*, vol.18, no.4, pp.1133-1145, DOI: 10.24507/ijicic.18.04.1133, 2022.
[9] C. I. Byrnes and A. Lindquist, *Theory and Applications of Nonlinear Control Systems*, Elsevier Science Pub. Co., New York, NY, USA, 1986.